Earth and Planetary Science
https://journals.nasspublishing.com/index.php/eps

REVIEW

Abiotic Oxygen Oases in Neoarchean Oceanic Large Igneous Provinces: A Hypothesis of Basalt Thermo-Acidolysis Triggered by Mantle Plume Redox Reactor

Alexandre de Oliveira Chaves

Institute of Geosciences, Federal University of Minas Gerais, Belo Horizonte 31270-901, Brazil

ABSTRACT

This paper suggested a conceptual, thermodynamically motivated hypothesis in which Neoarchean oceanic Large Igneous Provinces (LIPs) above oversized mantle plumes functioned as enormous abiotic oxygen reactors. In this framework, high heat flow and magmatic volatile fluxes (HCl, SO_2) drive pervasive thermo-acidolysis of oceanic lithosphere and oversized basaltic plateaus (oceanic LIPs), leading to slight water thermolysis, sulfur disproportionation, and local increases in oxygen fugacity toward the hematite-magnetite buffer (HM) within hydrothermal conduits. As an open system, progressive Fe exhaustion and advanced argillic alteration produce pyrophyllite-hematite-quartz linings that passivate conduit walls, while differential diffusion, degassing and rapid advection favour the kinetic survival of abiotic O_2 in an otherwise anoxic ocean, providing oxidative oases that preceded and possibly conditioned the emergence of biological oxygen production. The hypothesis yields testable predictions for thermodynamic-kinetic models and for the interpretation of hematite- and pyrophyllite-bearing alteration zones in Neoarchean greenstone belts. It is also suggested here that the precipitation of banded iron formations (BIFs), dolomitic carbonates and anhydrite was a spontaneous consequence of the basalt thermo-acidolysis. This process would have served as a precursor for the Paleoproterozoic Great Oxidation Event (GOE), contributing to generating the oxygen necessary to change the climate (Huronian Glaciation), the atmospheric chemistry (end of sulfur mass-

*CORRESPONDING AUTHOR:
Alexandre de Oliveira Chaves, Institute of Geosciences, Federal University of Minas Gerais, Belo Horizonte 31270-901, Brazil; E-mail: alex2010@ufmg.br

ARTICLE INFO
Received: 14 April 2026 | Revised: 9 July 2026 | Accepted: 28 July 2026 | Published Online: 7 August 2026
DOI: https://doi.org/10.36956/eps.v5i2.3253

CITATION
de Oliveira Chaves, A., 2026. Abiotic Oxygen Oases in Neoarchean Oceanic Large Igneous Provinces: A Hypothesis of Basalt Thermo-Acidolysis Triggered by Mantle Plume Redox Reactor. Earth and Planetary Science. 5(2): 1–14.
DOI: https://doi.org/10.36956/eps.v5i2.3253

independent fractionation, MIF-S), and the signature of life (Lomagundi-Jatuli $\delta^{13}C$ positive excursion).
Keywords: Neoarchean; LIP; Basaltic Oceanic Plateau; Volatiles; GOE; Abiotic Oxygen

1. Introduction

Understanding how and where oxidants accumulated on the early Earth is central to reconstructing the evolution of planetary redox state and the origins of aerobic metabolism [1]. A growing body of geochemical evidence suggests that Earth's oceans experienced localized and transiently oxygenated "oases" prior to the Great Oxidation Event (GOE) at ~2.4–2.3 Ga [2,3]. These oases are recorded by redox-sensitive trace metal distributions, Fe speciation, and sulfur isotopes, and are commonly interpreted as the result of spatially restricted oxygenic photosynthesis coupled to nutrient feedbacks, particularly phosphorus recycling [3,4].

In parallel, recent experimental and theoretical work has revitalized interest in abiotic sources of oxidants on the early Earth. Notably, it has been shown that abrasion of quartz grains in turbulent subaqueous environments can generate surface-bound radicals that oxidize water to produce hydrogen peroxide (H_2O_2), reactive oxygen species (ROS), and O_2 under strictly anoxic conditions, creating stable oxidant fluxes in near-shore and deltaic settings [5]. Such processes may have provided important oxidative niches and selection pressures prior to the evolution of oxygenic photosynthesis [1]. Additional models have explored abiotic Fe oxidation and ROS generation in hydrothermal and ferruginous settings [5,6]. The presence of hematite and other Fe(III) phases in some of the oldest greenstone belts and banded iron formations remains difficult to fully reconcile with a strictly reducing Archean ocean, especially when such minerals appear in association with hydrothermal alteration and silica-rich units [5,6]. These observations raise the question of whether part of the early Fe(III) record might reflect purely abiotic oxidation processes operating in unusual geodynamic contexts, rather than (or in addition to) localized biological O_2.

It is proposed herein that Neoarchean oceanic Large Igneous Provinces (LIPs) above oversize mantle plumes acted as gigantic abiotic oxygen reactors. The focus is on the interplay between thermo-acidolysis of basaltic plateaus by HCl–SO_2-rich fluids, the development of advanced argillic alteration, the exhaustion of Fe sinks, the H_2 escape to space and the kinetic survival of O_2 within a passivated hydrothermal setting. These processes could have created localized abiotic oxygen oases in the deep ocean, complementing shallow-water abiotic oxidant sources and biologically mediated oxygen oases. This contribution is intentionally conceptual, outlining the mechanism, connecting it to existing thermodynamic and geological constraints, and deriving testable predictions.

2. Neoarchean Oversize Mantle Plumes and Oceanic LIPs as Geochemical Reactors

Enormous volume mantle upwellings (oversized mantle plumes) can result from avalanches of 2.8 Ga hydrated oceanic plates that have sunk and accumulated at the lower mantle as slab graveyards. In the lower mantle, such slab graveyards became gravitationally unstable because water accumulated in them, which triggered oversize mantle plumes [7] that represent simultaneous mantle overturns (**Figure 1a**). Griffin et al. [8] suggest that there were one or more major 2.7 Ga mantle overturns (although they also suggest that potentially larger-scale mantle overturns may have occurred earlier), which were longer-lived and much larger than post-Archean plumes. Archean mantle potential temperatures were likely several hundred degrees Celsius higher than those of the modern mantle, fostering widespread plume activity and the formation of thick oceanic plateaus composed of basalts and, in earlier intervals, komatiites [9].

Based on geochemistry, Tomlinson and Condie [10] show that several Neoarchean greenstone belts are remnants of mantle plume-related oceanic plateus, named as the 2.85 Ga Fiskenaesset greenstone belt (South-West Greenland), the 2.71 Ga Lower Tisdale Group and the 2.71 Ga Stoughton-Roquemaure Group (Abitibi sub-

province, southern Superior Province, Canada), the 2.86 Ga Pickle Crow assemblage, the 2.7 Ga Wawa greenstone belt, and the 2.78 Ga Vizien greenstone belt (northern Superior Province, Canada). Puchtel et al.[11,12] have also proposed that the 3.0–2.8 Ga Kostomuksha and Sumozero-Kenozero Greenstone Belts of the Baltic Shield represent remnants of oceanic plateaus.

The Neoarchean oceanic plateaus would have experienced long-lived hydrothermal circulation with high water–rock ratios, driven by large thermal gradients and sustained magmatic volatile release (**Figure 1b**). Compared with modern plume settings (e.g., Hawaii, Iceland), Neoarchean mantle plumes likely combined higher magma temperatures, more reduced primary magmas, and larger fluxes of volatiles such as SO_2 and HCl[6,9].

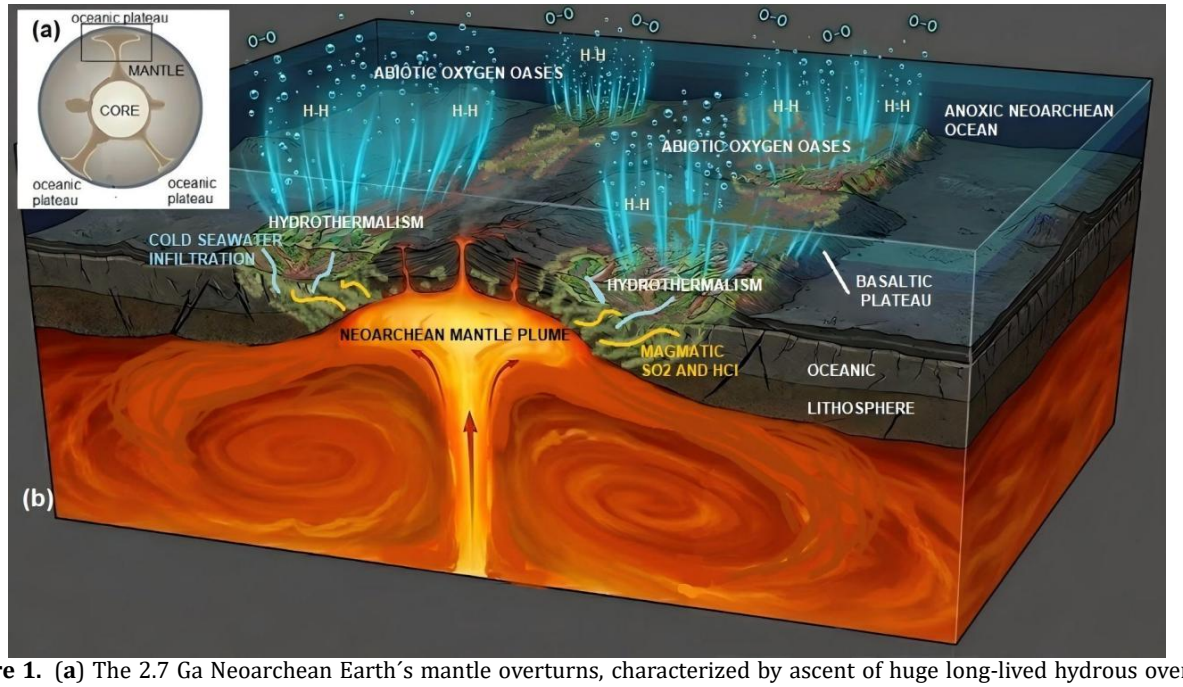

Figure 1. (**a**) The 2.7 Ga Neoarchean Earth´s mantle overturns, characterized by ascent of huge long-lived hydrous oversize mantle plumes from the Earth´s lower mantle, responsible for creation of (**b**) oceanic large igneous provinces represented by colossal basaltic plateaus. The pervasive hydrothermal activity caused by the constant interaction between the plume and the oceanic lithosphere and the basaltic plateau would have allowed the emergence of abiotic oxygen oases (figure not to scale).

In this context, basaltic oceanic plateau (Neoarchean LIP) and oceanic crust can be viewed as an oversize chemical reactor (**Figure 1b**) operating around 350 °C. Magmatic fluids ascend through a variably fractured basaltic pile, interacting with seawater-derived hydrothermal fluids and driving intense alteration, leaching and redox transformations in an open system. Modern analogues of advanced argillic alteration in volcanic systems demonstrate that strongly acidic, SO_2-rich and HCl-rich fluids can extensively strip cations and produce hematite and aluminous alteration assemblages at relatively shallow crustal levels[13]. This concept can be extended to Neoarchean oceanic basaltic plateaus, emphasizing the role of oversize mantle plume-driven heat and volatile fluxes in amplifying these processes according to the overall reaction (volcanic CO_2 was not included because it reacts with water to produce weak carbonic acid, which decomposes, resulting in the form of CO_2 and water, exactly as entered) of advanced argillic alteration of basalt:

$$\begin{aligned} &15Na_{0.4}Ca_{0.6}Al_{1.6}Si_{2.4}O_{8(s)} + \\ &10CaMg_{0.5}Fe_{0.5}Si_2O_{6(s)} + 5Fe_3O_{4(s)} + 5SO_{2(g)} \\ &+ 82HCl_{(aq)} + 12H_2O = 12Al_2Si_4O_{10}(OH)_{2(s)} \\ &+ 10Fe_2O_{3(s)} + 8SiO_{2(aq)} + 19Ca^{2+}{}_{(aq)} + 5Mg^{2+}{}_{(aq)} \\ &+ 5SO_4^{2-}{}_{(aq)} + 6Na^{+}{}_{(aq)} + 82Cl^{-}{}_{(aq)} + 38H^{+}{}_{(aq)} \\ &+ 6O_{2(g)} + 22H_{2(g)} \end{aligned} \quad (1)$$

Where, $Na_{0.4}Ca_{0.6}Al_{1.6}Si_{2.4}O_{8(s)}$—labradorite plagioclase; $CaMg_{0.5}Fe_{0.5}Si_2O_{6(s)}$—clinopyroxene; $Fe_3O_{4(s)}$—magnetite; $SO_{2(g)}$—sulfur dioxide; $HCl_{(aq)}$—hydrochloric

acid; H_2O—Water; $Al_2Si_4O_{10}(OH)_{2(s)}$—pyrophyllite; $Fe_2O_{3(s)}$—hematite; $SiO_{2(aq)}$—colloidal silica; $Ca^{2+}{}_{(aq)}$—ionic calcium; $Mg^{2+}{}_{(aq)}$—ionic magnesium; $SO_4{}^{2-}{}_{(aq)}$—ionic sulfate; $Na^{+}{}_{(aq)}$—ionic sodium; $Cl^{-}{}_{(aq)}$—ionic chloride; $H^{+}{}_{(aq)}$—ionic hydrogen; $O_{2(g)}$—abiotic oxygen gas; $H_{2(g)}$—hydrogen gas.

Emergence of the continents due to a global decrease in sea level and the growth of the continental crust during the Neoarchean produced a large amount of SO_2 in erupting magmas [14]. The subaerial to shallow-water topographic inflation of the oversize plateaus probably was a prerequisite to optimize the high SO_2 volatile fluxes required by the reaction 1.

The investigation of melt inclusions in olivine of Archean komatiites from 3.3 Ga to 2.7 Ga greenstone belts, made by Asafov et al. [15], shows that the enrichment in Cl and H_2O of the Earth's deep mantle originated from the subduction of the oceanic lithosphere previously altered by seawater. They argue that excessive Cl and H_2O concentrations in these komatiite sources were supplied into the hot and partially molten mantle plumes traversing the mantle transition zone. Therefore, SO_2 and HCl were indeed very important fluids in Neoarchean mantle plume-related magmatism.

Crucially, basaltic crust in the Neoarchean is volumetrically more important than komatiites [16] and contains higher bulk Al_2O_3 contents (~13–16 wt% versus ~4–7 wt% for komatiites), making it particularly conducive to forming thick pyrophyllitic seals under strongly acidic conditions at high temperature [17]. This compositional context suggests that basalt-dominated LIPs are statistically the most relevant substrates for widespread thermo-acidolysis and advanced argillic alteration in the Neoarchean.

Basaltic LIPs of oceanic plateaus are generated over mantle plumes by the sum of decompression melting at the plume head and the additional heat brought by the plumes. Mid-ocean ridge basalt (MORB) generation is conducted by the mechanism of decompression melting only (without heat involvement). Without intense heat, MORB setting could not produce comparable effects on abiotic oxygen production as suggested by reaction 1.

It must be emphasized that while Neoarchean greenstone belts preserve the thick basaltic sequences characteristic of plume-related volcanic architectures, they are not exact uniformitarian analogs to modern intraoceanic plateaus. Wu et al. [7] argue that the water-induced mantle overturns in the Neoarchean (**Figure 1a**) provide a large amount of water to induce hydrous melting at the base of the oceanic plateau to generate tonalite-trondhjemite-granodiorite (TTG) magmas. In this way, greenstone successions are commonly associated with granitoids, a feature absent in modern oceanic plateaus. However, this distinct petrological framework does not invalidate the proposed chemical reaction background.

3. Thermodynamic Basis: Sulfur Disproportionation, Water Thermolysis and Oxygen Fugacity (fO_2)

3.1. Sulfur Redox Cycling and Oxygen Fugacity

One key abiotic driver of oxidant generation in hydrothermal systems is the redox cycling of sulfur. At high temperature, disproportionation of magmatic SO_2 in water can produce sulfuric acid (H_2SO_4) and reduced sulfur (elemental liquid sulfur at 350 °C [18]), represented by the Equation (2) [13]:

$$3SO_{2(g)} + 2H_2O = 2H_2SO_{4(aq)} + S^0{}_{(liq)} \quad (2)$$

These are followed by dissociation of the strong sulfuric acid (H_2SO_4) on cooling, which yields H^+ ion and ionized aqueous-sulfate species represented in the Equation (3).

$$H_2SO_{4(aq)} = 2H^+{}_{(aq)} + SO_4^{2-}{}_{(aq)} \quad (3)$$

Ionic hydrogen attacks silicate reactants of the reaction 1 together with H^+ dissociated from hydrochloric acid of the Equation (4):

$$HCl_{(aq)} = H^+{}_{(aq)} + Cl^-{}_{(aq)} \quad (4)$$

The aggressive, nearly isochemical hydrolytic leaching of cations from the basaltic rock by the hyperacidic fluid (pH ~1 throughout reaction 1), leaves a siliceous residue with a vuggy texture [13]. The $38H^+$

on the product side of the reaction 1 simply represent the residual, unreacted excess acid required to sustain the hyperacidic environment.

Reactions (2) and (3) transfer oxidizing power from SO_2 to sulfate, raising local oxygen fugacity (fO_2) relative to mantle buffers. Equilibrium between magnetite and hematite provides a useful reference for the redox state of Fe-bearing minerals. At temperatures on the order of 350 °C, thermodynamic calculations place the magnetite–hematite (HM) buffer at fO_2 values several orders of magnitude above those characteristic of the reduced Archean mantle. The precise value depends on pressure, fluid composition and activities, but the critical point is that reaching or approaching HM conditions in a hydrothermal conduit implies a substantial local increase in oxidizing potential [6,19].

3.2. Water Thermolysis and H_2 Removal

At 350 °C and hydrothermal pressures, bulk water remains stable, but partial thermolysis and redox reactions at mineral surfaces can generate H_2 and reactive oxygen species, particularly in the presence of catalytic or radical-bearing surfaces [5,20]. The extent of this contribution in deep LIP hydrothermal systems is uncertain, but conceptually it can add to the oxidant budget generated by SO_2 disproportionation, especially where mineral surfaces promote dissociation or radical formation. McCollom et al. [21] suggest that H_2 production could be additionally developed by the Equation (5):

$$2Fe^{2+}_{(aq)} + 2H^{+}_{(aq)} = 2Fe^{3+}_{(aq)} + H_{2(g)} \quad (5)$$

A critical factor in sustaining high fO_2 is the fate of H_2. In a confined conduit, continuous removal of H_2 by degassing, diffusion into surrounding rocks or vent-proximal escape into the water column will bias the local redox state toward more oxidizing conditions [5,20]. Hydrogen's high diffusivity and low molecular weight favour its leakage through microfractures and porous media, whereas O_2 diffuses more slowly and may remain associated with the main fluid stream. It is suggested herein that the combination of SO_2 disproportionation, slight water thermolysis and effective H_2 removal allows confined segments of LIP hydrothermal systems to approach HM conditions, stabilizing hematite within an otherwise reduced Archean environment [6].

4. Advanced Argillic Alteration and the Formation of Pyrophyllite–Hematite–Quartz Conduits

Strongly acidic, high-temperature, sulfate- and chloride-rich fluids are known from modern volcanic systems to produce advanced argillic alteration, characterized by intense cation leaching and the development of mineral assemblages dominated by pyrophyllite and silica. Such alteration often forms lithocaps above magmatic-hydrothermal systems. In a Neoarchean oceanic LIP, similar fluids generated by SO_2-rich degassing and magmatic HCl release could interact with basaltic crust to produce vertically extensive zones of advanced argillic alteration [13,17].

Basalts with Al_2O_3 contents of 13–16 wt% can readily supply the Al necessary for pyrophyllite formation under highly acidic conditions, whereas Al-poor komatiites are less favourable for developing thick, continuous pyrophyllite horizons [16]. The reaction 1 shows that the fluid–rock interaction destroys plagioclase, clinopyroxene and magnetite, releasing Ca, Na, and Mg to the fluid while leaving behind an increasingly Al-rich residue. As fO_2 rises toward HM due to oxidant generation, Fe liberated from silicates and oxides is oxidized to Fe(III) and precipitated as hematite, while Al combines with silica and water to form pyrophyllite. Over time, the main fluid pathways evolve from basalt to a pyrophyllite–hematite–quartz assemblage.

This progression has two important consequences. First, the accessible reduced Fe along the conduit walls is progressively consumed, diminishing the capacity of the rock to buffer incoming oxidants. Second, the resulting mineral assemblage is mechanically competent and relatively inert, providing a structurally stable and chemically passivated lining for continued fluid flow [13]. In effect, advanced argillic alteration transforms reactive basalt into an "inert" pyrophyllite–silica structure, with hematite documenting the history of high fO_2 conditions. The reaction rate probably not decrease since the plume activity was pulsating during millions of years and new acidified basaltic layers were successively formed on

the oceanic plateau to sustain both the reaction 1 and the respective creation of passivation channels. When mantle plume activity was more intense and prolonged, basaltic melts eventually underwent magmatic differentiation processes, such as fractional crystallization, to produce dacitic and rhyolitic magmatic rocks in oceanic plateaus.

Neoarchean pyrophyllitic rocks ("agalmatolites") in the Rio das Velhas Greenstone Belt of the Brazilian Quadrilátero Ferrífero [22] as well as high-alumina alteration pipes underlying major BIF units in Australian Pilbara Craton [17] are the legacy of the basalt hydrothermal alteration process.

5. Mechanisms for Kinetic Survival of Abiotic O_2

5.1. Redox front Exhaustion and Passivation

The intuitive expectation that O_2 "dies at birth" in Archean hydrothermal systems stems from the enormous capacity of Fe^{2+}-rich rocks to titrate oxidants [5,6]. However, high-flux, long-lived fluid pathways can locally exhaust accessible Fe sinks, as observed in ore-forming systems where reaction fronts migrate and leave behind chemically depleted zones [13]. Once the dominant Fe reservoirs along the main fluid pathway are converted to Fe(III) or removed, the marginal oxygen demand of the rock declines sharply.

At this stage, additional oxidant-bearing fluids encounter a passivated, Fe-poor wall rock, and the net consumption of O_2 per unit fluid volume decreases. The redox front has effectively moved outward into surrounding basalt, leaving a core zone of exhausted Fe sinks. This "redox front exhaustion" creates a window in which oxidants can traverse the conduits with less reactive loss, increasing the probability that some O_2 survives advection to the seafloor.

5.2. Mineralogical Shielding and Catalytic Neutrality

Pyrophyllite and quartz differ fundamentally from Fe-bearing phases in their redox behaviour and catalytic properties. They are relatively inert to further oxidation [13] and do not provide abundant redox-active sites for H_2–O_2 recombination under hydrothermal conditions. By replacing basaltic wall rock with a pyrophyllite–silica lining, advanced argillic alteration not only depletes Fe but also removes many of the catalytic surfaces that would otherwise promote rapid O_2 consumption or recombination reactions.

It is proposed herein that the development of a continuous pyrophyllite–silica lining acts as a mineralogical shield, decoupling the interior of the fluid pathway from the large reduced Fe reservoirs in the surrounding crust. Diffusive exchange of O_2 and other oxidants into the wall rock is slowed by both mineralogical inertness and reduced reactive surface area. The fluid conduits thus evolve into chemically insulated channels in which oxidant-bearing fluids can be advected with comparatively low loss.

5.3. Differential Gas Transport, Advection and Quenching

Hydrogen's physical properties further bias the system toward net O_2 survival. H_2 is highly diffusive and can migrate rapidly through fractures, micro-porous media and into the atmosphere–ocean interface, whereas O_2 diffuses more slowly and may remain more strongly associated with the main fluid stream [5,20]. As a result, ascending fluids can become progressively more oxidizing in an effective sense, as H_2 escapes and oxidants remain.

Oversize mantle plume-driven systems provide strong thermal and buoyancy forces. Fluids at ~350 °C are less dense than surrounding rocks and overlying seawater, promoting rapid upward flow in permeable conduits. High flow velocities shorten the residence time of oxidant-bearing fluids in the most reactive segments of the conduit, reducing opportunities for complete O_2 consumption [5,6]. Upon discharge into much cooler Archean seawater, rapid quenching of the fluid temperature decreases reaction rates and may "freeze in" non-equilibrium O_2 and ROS abundances, analogous to the role of fast cooling in preserving metastable species in other geochemical contexts [1,5].

The kinetic survival and export of abiotic O_2

to seafloor vents do not depend on a uniformitarian, modern-style fluid regime, but are instead a predictable, systemic consequence of prolonged, plume-driven acid alteration. These three parameters—redox front exhaustion, mineralogical passivation, and high-velocity thermal advection—operate together as a self-reinforcing mechanism. Continuous thermoacidolysis progressively exhausts accessible Fe(II) sinks along the immediate conduit walls, migrating the active reaction front outward into the deeper crust. This exhaustion leaves behind a chemically inert, passivated lining of pyrophyllite and quartz that acts as a mineralogical shield, decoupling the ascending fluid stream from the surrounding reduced reservoirs. Propelled by the extreme buoyancy and steep thermal gradients generated by the underlying oversize mantle plume, the hyper-acidic fluid is rapidly advected through these insulated channels. This drastically shortens fluid residence times within the crust, ensuring that abiotic O_2 kinetically escapes recombination and is successfully preserved via thermal quenching upon discharge into the ocean.

6. Abiotic Oxygen Oases in the Context of Neoarchean Redox Evolution

Neoarchean marine sediments record multiple lines of evidence for spatially restricted, weakly oxygenated waters prior to the GOE, including Fe speciation patterns and trace metal distributions consistent with oxygenated surface or subsurface layers overlying ferruginous deep waters [2,3]. Recent modelling suggests that pulses of enhanced phosphorus recycling could have driven transient increases in biogenic O_2, creating dynamic oxygen oases whose existence was decoupled from global atmospheric oxygenation [3,4]. In parallel, experimental work on quartz abrasion has identified stable abiotic fluxes of H_2O_2 and O_2 in near-shore environments, providing oxidant sources that may have fostered oxygen tolerance and early aerobic metabolisms [5].

The model suggested herein adds a deep-ocean, extensive component to this heterogeneous redox landscape. Neoarchean mantle plume-related oceanic LIPs, with their high heat flow and volatile-rich magmatism, may have sustained long-lived hydrothermal systems capable of generating and exporting abiotic O_2 from below, producing oxygen oases centered on LIP-hosted vent fields. The absolute O_2 fluxes from such systems are expected to be small relative to later biological sources, but they would have generated steep local redox gradients in an otherwise strongly reduced ocean.

These gradients could have influenced pathways of Fe oxidation and banded iron formation, dolomite and anhydrite deposition, as well as the spatial distribution of oxidative stress and opportunities for the emergence of aerobic metabolisms in deep-water microbial communities. In this view, LIP-hosted abiotic oxygen oases complement shallow abiotic and biotic oxidant sources, collectively shaping a patchy Neoarchean redox landscape that predated the Great Oxidation Event (GOE).

7. Consequences of the Advanced Argillic Alteration of Neoarchean Basalts

The reaction 1 consumes magmatic silicates and produces H_2, abiotic oxygen (O_2) and a massive ionic charge, representing the "chemical recipe" for providing the necessary ingredients for the precipitation of the sedimentary and evaporitic rocks in the ocean. For banded iron formations (BIF), dolomite, and anhydrite to form, the reaction products would have had to be transported through hydrothermal systems, such as fumaroles (smokers), to the oceanic basin.

7.1. Formation of BIFs (Banded Iron Formations) and Ocean Salinity

The BIFs would essentially be a physical recording of the oversized mantle plume's internal pressure cycles. The connection between the intense Neoarchean mantle plume activity and BIF deposition is evident when analyzing **Figure 2a**,**b** together. A Neoarchean BIF is defined by its rhythmic, millimeter-to-centimeter-scale layering of iron oxide (mainly magnetite [23]) and microcrystalline silica (chert, SiO_2). The mechanical explanation for these bands would be based on the pulsatory activity of the oversized mantle plume during its activity over

millions of years. Equation (6) is the step of magnetite formation in Neoarchean BIFs:

$$6Fe^{2+}_{(aq)} + O_{2(g)} + 6H_2O = 2Fe_3O_{4(s)} + 12H^{+}_{(aq)} \quad (6)$$

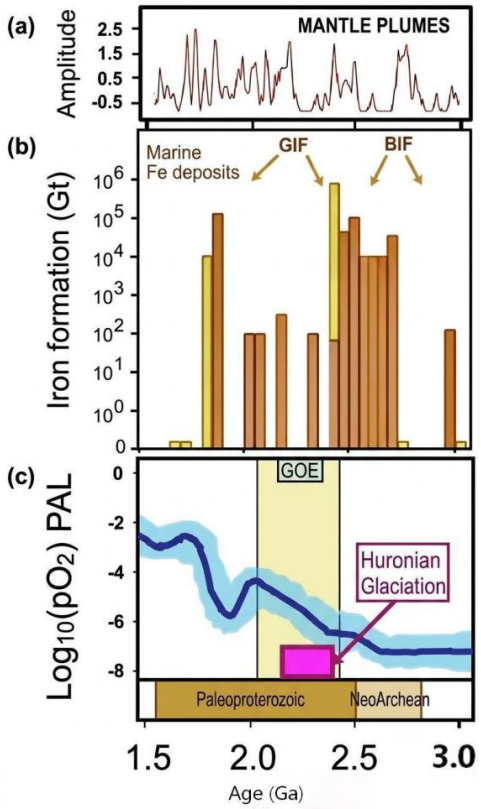

Figure 2. (**a**) Distribution (amplitude) of mantle plumes from 3.0 Ga to 1.5 Ga, developed in this study based on the LIP Age Database (version 2016 [24]). (**b**) Distribution of marine Fe deposits plotted as amount of iron formation in billion metric tons (Gt) from 3.0 to 1.5 Ga [25]. (**c**) Quantitative prediction of atmospheric O_2 content using machine learning, relative to the present atmospheric level (PAL) from 3.0 to 1.5 Ga, with analytical errors represented in blue [26]. Purple bar represents the time interval of the Huronian Glaciation [27].

Note: BIF—banded iron formation; GIF—granular iron formation; GOE—Great Oxidation Event. The Continuous Wavelet Transform was applied to the histogram signal of **Figure 2a**. Unlike the Fourier Transform, the Wavelet decomposes the signal both in time (age) and scale (approximate frequency). The Mexican Hat wavelet was used (also known as the Ricker wavelet), which is the second derivative of a Gaussian function. It is ideal for geosciences because it is excellent at detecting isolated peaks.

$$\psi(t) = \frac{2}{\sqrt{3\sigma}\pi^{\frac{1}{4}}}(1 - (\frac{t}{\sigma})^2)e^{-\frac{t^2}{2\sigma^2}}$$

The transform W for a scale "a" and position "b" was calculated by convolving the histogram signal f(t) with the translated and scaled wavelet:

$$W(a,b) = \frac{1}{\sqrt{|a|}}\int_{-\infty}^{\infty} f(t)\psi^*(\frac{t-b}{a})dt$$

Where ψ^* denotes the complex conjugate of the wavelet function.
The 10 Ma uncertainty histogram (data has been processed using a temporal window of 10 million years—this accounts for dating errors and prevents the histogram from showing artificial, jagged spikes caused purely by analytical scatter rather than real geological history) was treated as a discrete one-dimensional signal f(t). Coefficients were calculated for scales from 1 to 15, where smaller scales detect noise and rapid individual events, and larger scales detect large groupings or magmatic cycles.

The abiotic oxygen released by reaction 1 meets soluble ionic Fe^{2+} from pre-existing Neoarchean seawater, precipitating as magnetite. This is the "dark band." As also established in reaction 1, the destruction of basalt releases massive amounts of dissolved silica. The silica precipitates as a colloidal gel after its saturation, which later hardens into chert. This is the "white band." The alternation between these two phases (magnetite and silica) creates the characteristic banding.

The escape of sodium and chlorine would have resulted in the injection of tons of Na^+ and Cl^- into seawater, and ocean salinity would have reached modern levels possibly in the Neoarchean, coinciding with massive activity of the plumes and the emergence of BIFs.

7.2. Formation of Dolomite [$CaMg(CO_3)_2$]

The reaction also releases exactly the two necessary cations for the formation of dolomite: Ca^{2+}, Mg^{2+}. In the open marine environment, where there are available bicarbonate ions, increased pH favors its precipitation following the Equation (7):

$$Ca^{2+}_{(aq)} + Mg^{2+}_{(aq)} + 2HCO^{-}_{3\ (aq)} = CaMg(CO_3)_{2(s)} + 2H^{+}_{(aq)} \quad (7)$$

The released H^+ reacts rapidly with another bicarbonate ion from the ocean (Equation (8)):

$$H^{+}_{(aq)} + HCO^{-}_{3\ (aq)} = CO_{2(g)} + H_2O_{(liq)} \quad (8)$$

This means that the formation of dolomite ends up releasing carbon dioxide (CO_2) into the ocean, which helps to balance its acidity. In many Neoarchean cratons (such as the Hamersley Basin in Australia or the Transvaal Basin in South Africa), BIFs and dolomites are often found in close stratigraphic proximity [23]. This vertical succession reflects the changing ocean chemistry and the rise of atmospheric oxygen.

7.3. Formation of Anhydrite ($CaSO_4$)

A large excess of Ca^{2+} and $SO_4{}^{2-}$ (sulfate) results from the reaction 1. In a marginal oceanic basin, the concentration of these ions reaches the solubility product and anhydrite is formed (Equation (9)):

$$Ca^{2+}_{(aq)} + SO^{2-}_{4\ (aq)} = CaSO_{4(s)} \quad (9)$$

Increasing spread in the pyrite $\delta^{34}S$ values from the Neoarchean to the early Paleoproterozoic characterizes this marked increase in the concentration of sulfate in seawater [28] promoted by reaction 1.

8. MIF-S, Carbon-13 (Isotopic Fingerprints) and Global Cooling

The reaction 1 acts as a true Neoarchean geochemical engine. It describes the alteration of primary minerals (pyroxene, plagioclase and magnetite) by extremely aggressive acidic fluids to produce abiotic oxygen, connecting the ancient lithosphere, atmosphere, and biosphere. Apparently, this reaction repeated itself around 2.5–2.4 Ga, as revealed by the peak of mantle plume activity and the corresponding large amount of BIF deposition (now richer in hematite [23]) at the beginning of the Paleoproterozoic (**Figure 2a**,**b**).

As illustrated in **Figure 2a**, compiled from the updated global LIP Age Database [24], the continuous wavelet transform analysis indeed reveals prominent, high-amplitude magmatic peaks concentrated between 2.5 Ga and 2.4 Ga (e.g., the massive Matachewan plume/dyke swarm and related crustal events [29]). This precise interval marks the transitional threshold where newly stabilized Neoarchean cratons were subjected to major plume-induced rifting and volcanic margins before the 2.4–2.2 Ga interval of deep magmatic shutdown (shown in **Figure 2a**) took full effect. The 2.5–2.4 Ga interval directly coincides with the absolute global peak in the depositional volume of Banded Iron Formations (BIFs), such as those in the Hamersley (Australia) and Transvaal (South Africa) basins [23], which are increasingly richer in hematite.

The ongoing cratonization process actually facilitated the subaerial emergence of extensive continental blocks and thick volcanic plateaus inflated by oversize plumes. This topographic transition is essential to the abiotic O_2 model, as it shifted the volcanic degassing regime from a low-pressure subaqueous environment to a subaerial/shallow-water setting, which significantly increased the flux of SO_2 relative to H_2S [14], accelerating the proposed thermoacidolysis reactor. The proposed abiotic mechanism does not replace established surficial or biogenic models but acts as a transient, deep-seated geochemical trigger during the major magmatic pulses of the Neoarchean-Paleoproterozoic transition.

8.1. The Lomagundi-Jatuli Event

The Lomagundi-Jatuli event is characterized by a massive positive excursion of $\delta^{13}C$ in carbonates from 2.4 Ga to 2.1 Ga. The simultaneous release of nutrients (such as Mg^{2+} and Fe^{2+}) and abiotic O_2 from the reaction 1 would stimulate organic productivity. Burying this excess generated organic matter "cleans" the ^{12}C from the system, leaving the carbonates enriched in ^{13}C [30].

There is a direct correlation between the burial of organic carbon and the oxygenation of the planet

(**Figure 2c**). For every atom of organic carbon that is buried and does not undergo oxidation (decomposition), one molecule of free oxygen (O_2) remains in the atmosphere. Therefore, large positive $\delta^{13}C$ anomalies in the geological record (such as the Lomagundi-Jatuli event in the Paleoproterozoic) are interpreted as periods of significant oxygenation of the Earth [30].

The Neoarchean mantle overturns injected vast amounts of mantle-derived CO_2, which was sequestered by the massive dolomite platforms, potentially cooling the planet, setting the climatic stage for the Great Oxidation Event (GOE—**Figure 2c**) and modulating the global carbon cycle during the intense volcanic activity.

8.2. The End of MIF-S (Sulfur Mass-Independent Fractionation)

In the Archean, the atmosphere lacked an ozone layer, allowing solar ultraviolet (UV) radiation to strike atmospheric volcanic gases such as SO_2. This caused Mass-Independent Fractionation (MIF-S), a unique signature expressed by values of $\Delta^{33}S \neq 0$. With the activity of oceanic LIPs, magmatic sulfur (which possesses Mass-Dependent Fractionation or MDF, with $\Delta^{33}S \approx 0$) was injected into the system, diluting the sulfur that originated from the atmosphere. As the reaction 1 releases free O_2, oxygen begins to accumulate in the atmosphere. This O_2 contributes to forming the ozone layer (O_3), which blocks the UV radiation necessary for MIF-S. Furthermore, oxygen rapidly oxidizes atmospheric sulfur species to soluble sulfates. As a result, the geological record stops showing MIF-S anomalies, marking the transition between Neoarchean and Paleoproterozoic as the exact moment when the atmosphere became oxidizing [30].

8.3. The 2.3–2.2 Ga Huronian Glaciation

In the Archean atmosphere, methane gas (CH_4) was the main warming gas [15]. The O_2 produced by reaction 1 would react with methane, transforming it into CO_2 (a much less potent greenhouse gas) and water. In addition, the new abundance of oceanic sulfate provided a feast for primitive Sulfate-Reducing Bacteria (SRB). These organisms used the plume's sulfate generated by reaction 1 to oxidize methane (CH_4) in the water column. This began the slow "chipping away" at the methane greenhouse, a process that would culminate in the global freeze. Without methane, the Earth loses its thermal "blanket." The temperature plummets, triggering the advance of glaciers and the Snowball Earth cycle that characterizes the Huronian Glaciation (**Figure 2c**) described by Kurucz et al. [27].

9. Testable predictions and implications

Although this contribution is intentionally limited to a conceptual hypothesis, it yields several testable predictions.

9.1. Thermodynamic–Kinetic Feasibility of HM Level fO_2 in LIP Conduits

Reactive transport and equilibrium modeling of basalt–HCl–SO_2–H_2O systems at Neoarchean Pressure–Temperature–Composition conditions should demonstrate that confined, high-flux conduits can approach HM fO_2 when strong SO_2 fluxes and continuous H_2 removal are imposed, and should quantify the resulting O_2 and sulfate abundances.

9.2. Development of Pyrophyllite–Hematite–Quartz Linings and Fe Exhaustion

Models should reproduce the evolution from basaltic wall rock to pyrophyllite–hematite–quartz assemblages along major pathways under high acidity and oxidant fluxes, and should resolve the spatial migration of redox fronts and Fe depletion.

9.3. Redox Signatures in Neoarchean Alteration Zones and BIFs

Comparative studies of Neoarchean greenstone belts and associated Iron Formations should assess whether specific hematite and pyrophyllite-bearing alteration zones display geochemical and isotopic signatures consistent with abiotic hydrothermal oxidation, distinguishing them from solely biogenic or metamorphic Fe(III).

9.4. Integration with Shallow Abiotic Oxidant Sources

Quantitative models of early Earth redox evolution should incorporate both deep LIP-hosted oxidant fluxes and shallow quartz abrasion-driven H_2O_2/O_2 fluxes, evaluating their combined capacity to generate oxidative niches and to influence Fe cycling and nutrient dynamics.

9.5. Constraints from Early Biogeochemical Proxies

If LIP-hosted abiotic oxygen oases were significant, some Neoarchean redox proxies might record deep water or midwater oxygenation events spatially associated with LIP provinces, potentially detectable through regional correlations of Fe speciation, REE + Y patterns and S isotopes.

10. Discussion

The reactor model requires a powerful thermal driver to facilitate the thermoacidolysis of basalt. Barley et al.[31] provide the essential framework for this, describing the Neoarchaean bonanza as a period of profound metallogenic and environmental consequences driven by the interaction of mantle plumes with lithospheric tectonics. These authors suggest that Neoarchean LIPs were the product of global-scale plume activity. These plumes provided the sustained, high-volume magmatic flux and the thermal gradients necessary to drive hydrothermal systems. In the context of the mantle plume redox model, the bonanza[31] represents the intense hydrothermal throughput required to drive the reaction 1. This provides a clear link between mantle plume dynamics and the localized generation of oxidative oases.

The hypothesis that Neoarchean greenstone belts—as remnants of plume-related oceanic Large Igneous Provinces (LIPs)—functioned as immense abiotic oxygen reactors is supported by the records of several type-localities. The Abitibi greenstone belt (Canada) serves as an example of a reactor in this model due to its vast, well-preserved accumulation of volcanic sequences and extensive VMS (Volcanogenic Massive Sulfide) deposits. The Abitibi is a remnant of a mantle plume-related oceanic plateau[10], and its intense hydrothermal footprints, specifically those at LaRonde-Bousquet 2[32], demonstrate the pervasive advanced argillic alteration predicted by the mantle plume redox model.

By identifying Belingwe greenstone belt as a remnant of an Archean oceanic plateau, Kusky and Kidd[33] validated the stratigraphic continuity necessary for large-scale fluid channeling. This structural preservation reveals that this plateau was not subjected to the intense dismemberment seen in later orogenic processes, allowing it to function as a coherent, long-lived conduit.

Many Neoarchean tholeiites have geochemical signatures very similar to those of Phanerozoic oceanic plateaus, and it is widely considered that oceanic plateaus are their closest analogues. This has led to proposals that many Neoarchean greenstones formed as plume-related oceanic plateaus, and that continents grew in part through docking of such oceanic plateaus[34–37]. The convergence of these lines of evidence indicates that the reactor model is not merely a theoretical construct but a logical consequence of Archean geodynamics.

Crucially, the thermodynamic feasibility of this thermoacidolysis reactor is predicated on the large amount of HCl and SO_2 within the magmatic volatile flux. Asafov et al.[15] argue that excessive Cl and H_2O concentrations in Neoarchean komatiite sources were supplied into the hot and partially molten mantle plumes, suggesting that HCl was an important volatile phase in such plumes. The eruption of the plume-related Siberian Traps is estimated to have released 68 billion tons of SO_2 over less than 1 million years, and S isotope compositions of melt inclusions indicate that most of this sulfur was mantle derived[38]. This amount from the 250 Ma Siberian eruption may suggest that SO_2 emissions associated with Neoarchean plumes were equivalent or even greater.

The Neoarchean development of massive oceanic plateaus—and their subsequent shallowing—facilitated rapid, decompression-driven eruptions. This tectonic transition toward shallow-water and subaerial volcanism inherently promotes the discharge of SO_2[14], creating the hyper-acidic conditions essential to catalyze the

intensive thermoacidolysis of basaltic lithologies. SO_2 predominates in high-temperature (~1,200 °C) shallow-water and subaerial emissions because thermodynamic equilibrium favors the formation of small molecules, like H_2. Hence, H_2S gas reacts with water to produce sulfur dioxide and hydrogen gases, according to Equation (10) [39].

$$H_2S_{(g)} + 2H_2O = SO_{2(g)} + 3H_{2(g)} \quad (10)$$

Consequently, the growth of these Neoarchean LIPs did not merely provide the structural plumbing for fluid circulation; it acted as a geochemical trigger, shifting the volatile output toward the high-flux HCl and SO_2 environment necessary to drive the reaction 1. This mechanism accounts for both the advanced argillic alteration zones observed in the geological record and the local oxygen fugacity increases required for abiotic O_2 production. Thus, the intersection of plume-driven thermal gradients and volatile degassing suggests that these volcanic centers operated as self-sustaining, planetary-scale chemical engines, providing oxidative oases in the Neoarchean ocean.

At 350 °C, the reaction 1 could be spontaneous since its Gibbs Free Energy (ΔG) is probably driven negative by two main factors: (a) Entropic Gain—the generation of 28 moles of gas ($22H_2$ + $6O_2$) from liquid and solid phases significantly increases system entropy and (b) Enthalpic Drive—the extreme acidity (H_2SO_4 and HCl) and the oxidation of magnetite to hematite release the energy required for the slight dissociation of water molecules into gaseous O_2 and H_2. In fact, under standard hydrothermal conditions of 350 °C, water dissociation is small. However, in an oversize mantle plume, the thermal gradient at the base of the hydrothermal system can reach temperatures where dissociation becomes kinetically relevant for releasing both gases.

11. Conclusions

The proposed reaction 1 represents a redox engine for the early Earth. By transforming reduced basalt into oxidized hematite and inert pyrophyllite, oversize mantle plumes acted as abiotic oxygen reactors. This model reduces the dependency on biological evolution as the sole driver of the GOE and provides a unified framework for understanding the link between deep mantle dynamics and surface environmental revolutions developed during the transition Archean-Proterozoic.

The hypothesis presented herein proposes that Neoarchean oceanic LIPs (oceanic plateaus) above oversized mantle plumes functioned as important abiotic oxygen reactors, generating localized oxygen oases through thermoacidolysis, sulfur disproportionation, Fe sink exhaustion and kinetic survival of O_2 in passivated hydrothermal conduits. This mechanism is intended to complement, not replace, established models of shallow abiotic oxidant production and biogenic oxygen oases. It offers a geodynamically plausible, thermodynamically grounded framework for interpreting some early Fe(III) signatures and for understanding the diversity of oxidative niches prior to the GOE [1,3,5,6].

Since the present work is purely conceptual, its value lies in guiding future quantitative studies and suggesting new observational targets. If supported by modeling and field evidence, LIP-hosted abiotic oxygen oases may represent an important, previously underappreciated component of Earth's early redox architecture.

Funding

This work was supported by a research productivity grant from CNPq (Brazilian Science and Technology Agency).

Institutional Review Board Statement

Not applicable.

Informed Consent Statement

Not applicable.

Data Availability Statement

The data are available in the paper body.

Acknowledgments

Thanks to the authors and the Society of Economic Geologists for the permission to use **Figure 2b** available at https://pubs.geoscienceworld.org/segweb/economicgeology/article/105/3/467/128197/Iron-Formation-The-Sedimentary-Product-of-a. Thanks to the authors of **Figure 2c** from Nature Communications and to Springer Nature for the permission to use the modified version of this figure, available at https://www.nature.com/articles/s41467-022-33388-5, which is licensed under a Creative Commons Attribution 4.0 International License, which permits use, sharing, adaptation, distribution and reproduction in any medium or format. Thanks to the reviewers for their comments and suggestions, which contributed to improving the article.

Conflicts of Interest

The author declares no conflict of interest.

AI Use Statement

During the preparation of this work, the author used Perplexity AI to review the text and to improve the English language. After using this tool/service, the author reviewed and edited the content as needed and takes full responsibility for the content of the published article.

References

[1] Ślesak, I., Ślesak, H., Kruk, J., 2012. Oxygen and hydrogen peroxide in the early evolution of life on earth: In silico comparative analysis of biochemical pathways. Astrobiology. 12(8), 775–784. doi: https://doi.org/10.1089/ast.2011.0704

[2] Anbar, A.D., Duan, Y., Lyons, T.W., et al., 2007. Whiff of oxygen before the great oxidation event? Science. 317(5846), 1903–1906. doi: https://doi.org/10.1126/science.1140325

[3] Cañadas, F., Guilbaud, R., Fralick, P., et al., 2025. Archaean oxygen oases driven by pulses of enhanced phosphorus recycling in the ocean. Nature Geosciences. 18(5), 430–435. doi: https://doi.org/10.1038/s41561-025-01678-4

[4] Reinhard, C.T., Planavsky, N.J., Lyons, T.W., 2013. Long-term sedimentary recycling of rare sulphur isotope anomalies. Nature. 497(7447), 100–103.

[5] He, H., Wu, X., Xian, H., et al., 2021. An abiotic source of Archean hydrogen peroxide and oxygen that pre-dates oxygenic photosynthesis. Nature Communications. 12(1), 6611.

[6] Dodd, M.S., Wang, H., Li, C., et al., 2022. Abiotic anoxic iron oxidation, formation of Archean banded iron formations, and the oxidation of early Earth. Earth and Planetary Science Letters. 584, 117469.

[7] Wu, Z., Song, J., Zhao, G., et al., 2023. Water-induced mantle overturns leading to the origins of Archean continents and subcontinental lithospheric mantle. Geophysical Research Letters. 50(22), e2023GL105178. doi: https://doi.org/10.1029/2023GL105178

[8] Griffin, W.L., Belousova, E.A., O'Neill, C., et al., 2014. The world turns over: Hadean–Archean crust–mantle evolution. Lithos. 189, 2–15.

[9] Herzberg, C., Condie, K., Korenaga, J., 2010. Thermal history of the Earth and its petrological expression. Earth and Planetary Science Letters. 292(1–2), 79–88.

[10] Tomlinson, K.Y., Condie, K.C., 2001. Archean mantle plumes: Evidence from greenstone belt geochemistry. In: Ernst, R.E., Buchan, K.L. (Eds.). Mantle Plumes: Their Identification through Time, Geological Society of America Special Paper 352. Geological Society of America: Boulder, CO, USA. pp. 341–357.

[11] Puchtel, I.S., Hofmann, A.W., Mezger, K., et al., 1998. Oceanic plateau model for continental crustal growth in the Archaean: A case study from the Kostomuksha greenstone belt, NW Baltic Shield. Earth and Planetary Science Letters. 155(1/2), 57–74.

[12] Puchtel, I.S., Hofmann, A.W., Amelin, Y.V., et al., 1999. Combined mantle plume-island arc model for the formation of the 2.9 Ga Sumozero-Kenozero greenstone belt, SE Baltic Shield: Isotope and trace element constraints. Geochimica et Cosmochimica Acta. 63(21), 3579–3595.

[13] Hedenquist, J.W., Arribas, A., 2022. Exploration implications of multiple formation environments of advanced argillic minerals. Economic Geology. 117(3), 609–643.

[14] Gaillard, F., Scaillet, B., Arndt, N.T., 2011. Atmospheric oxygenation caused by a change in volcanic degassing pressure. Nature. 478, 229–233.

[15] Asafov, E.V., Sobolev, A.V., Batanova, V.G., et al., 2020. Chlorine in the Earth's Mantle as an Indicator of the Global Recycling of Oceanic Crust. Russian Geology and Geophysics. 61(9), 937–950.

[16] Puchtel, I.S., Blichert-Toft, J., Horan, M.F., et al., 2022. The komatiite testimony to ancient mantle heterogeneity. Chemical Geology. 596, 120776.

[17] Brenner, A.R., Fu, R.R., Brown, A.J., et al., 2024. Episodic seafloor hydrothermal alteration as a source of stable remagnetizations in Archean volcanic rocks. Geochemistry, Geophysics, Geosystems. 25(12), e2024GC011799. doi: https://doi.org/10.1029/2024GC011799

[18] Dekov, V.M., Koschinsky, A., Yamanaka, T., et al., 2024. Native sulfur at the seafloor: Composition and origin. Chemical Geology. 668, 122295. doi: https://doi.org/10.1016/j.chemgeo.2024.122295

[19] Kress, V.C., Carmichael, I.S.E., 1991. The compressibility of silicate liquids containing Fe_2O_3 and the effect of composition on their redox states. Contribution to Mineralogy and Petrology. 108, 82–92.

[20] Catling, D.C., Zahnle, K.J., 2020. The Archean atmosphere. ScienceAdvances. 6(9), eaax1420. doi: https://doi.org/10.1126/sciadv.aax1420

[21] McCollom, T.M., Robbins, M., Moskowitz, B., et al., 2013. Experimental study of acid-sulfate alteration of basalt and implications for sulfate deposits on Mars. Journal of Geophysical Research: Planets. 118(4), 577–614. doi: https://doi.org/10.1002/jgre.20044

[22] Romano, A.W., Araújo, C., 2018. Agalmatolite and talc. In: Pedrosa-Soares, A.C., Voll, E., Cunha, E.C. (Eds.). Mineral Resources of Minas Gerais Online: A Synthesis of Knowledge about the Mineral Wealth, Geological History, and Environment and Mining of Minas Gerais. Companhia de Desenvolvimento de Minas Gerais (CODEMGE): Belo Horizonte, Brazil. Available from: http://recursomineralmg.codemge.com.br/wp-content/uploads/2018/10/Agalmatolito.pdf (in Portuguese)

[23] Trendall, A.F., 2002. The significance of Iron-Formation in the Precambrian stratigraphic record. In: Altermann, W., Corcoran, P.L. (Eds.). Precambrian Sedimentary Environments. Blackwell Science: Oxford, UK. pp. 33–66. doi: https://doi.org/10.1002/9781444304312.ch3

[24] Large Igneous Provinces Commission, 2016. LIP Age Database: Global listing in Spreadsheet Format (version: 30 October 2016). Available from: http://www.largeigneousprovinces.org/downloads (cited 4 April 2026).

[25] Bekker, A., Slack, J.F., Planavsky, N., et al., 2010. Iron Formation: The Sedimentary Product of a Complex Interplay among Mantle, Tectonic, Oceanic and Biospheric Processes. Economic Geology. 105, 467–508.

[26] Chen, G., Cheng, Q., Lyons, T.W., et al., 2022. Reconstructing Earth's atmospheric oxygenation history using machine learning. Nature Communications. 13, 5862. doi: https://doi.org/10.1038/s41467-022-33388-5

[27] Kurucz, S., Fralick, P., Homann, M., et al., 2021. Earth's first snowball event: Evidence from the early Paleoproterozoic Huronian Supergroup. Precambrian Research. 365, 106408. doi: https://doi.org/10.1016/j.precamres.2021.106408

[28] Kump, L.R., 2012. Sulfur isotopes and the stepwise oxygenation of the biosphere. Elements. 8(6), 410–411. doi: https://doi.org/10.2113/gselements.8.6.410

[29] Ciborowski, T.J.R., Kerr, A.C., Ernst, R.E., et al., 2015. The Early Proterozoic Matachewan Large Igneous Province: Geochemistry, petrogenesis, and implications for Earth evolution. Journal of Petrology. 56(8), 1459–1494.

[30] Lyons, T.W., Reinhard, C.T., Planavsky, N.J., 2014. The rise of oxygen in Earth's early ocean and atmosphere. Nature. 506(7488), 307–315.

[31] Barley, M.E., Krapez, B., Groves, D.I., et al., 1998. The Late Archaean bonanza: Metallogenic and environmental consequences of the interaction between mantle plumes, lithospheric tectonics and global cyclicity. Precambrian Research. 91(1–2), 65–90.

[32] Dubé, B., Mercier-Langevin, P., Kjarsgaard, I., et al., 2014. The Bousquet 2-Dumagami World-Class Archean Au-Rich volcanogenic massive sulfide deposit, Abitibi, Quebec: Metamorphosed submarine advanced argillic alteration footprint and genesis. Economic Geology. 109(1), 121–166.

[33] Kusky, T.M., Kidd, W.S.F., 1992. Remnants of an Archean oceanic plateau, Belingwe greenstone belt, Zimbabwe. Geology. 20(1), 43–46.

[34] Kerr, A.C., White, R.V., Saunders, A.D., 2000. LIP reading, recognizing oceanic plateaux in the geological record. Journal of Petrology. 41(7), 1041–1056.

[35] Condie, K.C., 2005. High field strength element ratios in Archean basalts: A window to evolving sources of mantle plumes? Lithos. 79(3–4), 491–504.

[36] Ernst, R.E., Buchan, K.L., 2003. Recognizing mantle plumes in the geological record. Annual Review of Earth and Planetary Sciences. 31, 469–523.

[37] Kerrich, R., Polat, A., 2006. Archean greenstone-tonalite duality: Thermochemical mantle convection models or plate tectonics in the early Earth global dynamics? Tectonophysics. 415(1–4), 141–165.

[38] Wallace, P.J., Plank, T., Edmonds, M., et al., 2015. Volatiles in magmas. In: Sigurdsson, H., Houghton, B., McNutt, S., et al. (Eds.). The Encyclopedia of Volcanoes, 2nd ed. Academic Press: Cambridge, MA, USA. pp. 163–183.

[39] Catling, D.C., Kasting, J.F., 2017. Atmospheric Evolution on Inhabited and Lifeless Worlds. Cambridge University Press: Cambridge, UK.